15 July 1994

OPTICS COMMUNICATIONS

ELSEVIER

Optics Communications 109 (1994) 400–404

Multiplexing interrogation of interferometric sensors using dual multimode laser diode sources and coherence reading

A.B. Lobo Ribeiro [1], Y.J. Rao, D.A. Jackson

Applied Optics Group, Physics Laboratory, University of Kent, Canterbury, Kent CT2 7NR, UK

Received 23 June 1993; revised manuscript received 17 January 1994

Abstract

A multiplexing topology with virtually no cross-talk is demonstrated for a sensor network based upon low coherence interferometry, in which a scanning interferometer simultaneously interrogates all the sensors. Dual wavelength operation using two multimode laser diode sources is implemented. The concept is demonstrated by multiplexing two bulk optical Michelson interferometers. For both sensors the achieved resolution was of the order of 1 nm, with a working range of 45 μm.

1. Introduction

Low coherence interferometry offers the possibility of solving the 'powering up' problem associated with all fibre optic interferometric sensors used to measure slowly varying measurands, such as temperature or displacement. In a typical system, the remote sensor is illuminated with the output from a source with low temporal coherence, and interrogated using a second interferometer which is scanned in such a way that its optical path difference (OPD) is matched to that of the sensor [1]. For fibre optic sensors to compete with conventional electric sensors, it is desirable to be able to multiplex several sensors. A variety of multiplexing configurations for interferometric sensors, exploiting low coherence processing, have been developed, which include coherence tuning [2] and time division multiplexing (TDM) [3]. Practical difficulties are experienced with both techniques. The main problems with coherence tuning are: (i) the optical path lengths of the sensors must be all different from each other (within the source coherence length), which imposes restrictions on sensor design, particularly in the case of a network with miniature sensors; (ii) very high noise levels, because the recovered signal contains both the desired signal from the sensor as well as partially uncorrelated optical power from all other sensors in the network, which inevitably results in poor signal-to-noise ratios (SNR). The noise associated with the uncorrelated signals can be eliminated by implementing TDM; however, as it is necessary to sequentially coherence match the local receiving interferometer (LRI) to each sensor, the technique is difficult to use in practice.

Here we report a novel partially multiplexed configuration using a demodulation technique based on dual-wavelength signal processing, where the problems referred to above can be avoided by fully multiplexing the scanning interferometer and the signal processing unit, whilst at the same time, the sensor network is partially multiplexed. With this network topology, significant advantages are achieved: (i)

[1] INESC, Optoelectronics Center, R. José Falcão 110, 4000 Porto, Portugal.

0030-4018/94/$07.00 © 1994 Elsevier Science B.V. All rights reserved
SSDI 0030-4018(94)00208-C

there is virtually no cross-talk, and the optical power is used much more effectively because the optically encoded output signal from each sensor is returned directly to a separate detector via a dedicated optical fibre link, rather than using the fibre network to distribute the optical power to each sensor; (ii) with the selected demodulation scheme the operational range of each sensor can be equal to the effective wavelength of the dual wavelength source (λ_e); (iii) the range of each sensor is unaffected by the number of sensors in the system.

2. Principle

The system is illuminated by two low coherence optical sources (LCOS), with mean wavelengths λ_1 and λ_2, and exploits a two-wavelength, classical demodulation technique to determine the phase excursion of each interferometric sensor. By using this approach, the absolute value of the measurand field is determined within a much wider unambiguous range when the sensor is initialized. This method of signal processing has been previously demonstrated [4] for a single fibre optic sensor. The difference in the phase shift measured at each wavelength (λ_1 and λ_2) is a function of the sensor OPD, and exhibits an unambiguous range ($\pm\pi$). This range depends on the actual wavelength difference ($\lambda_1 - \lambda_2$) and can exceed more than ± 100 individual interferometric fringes in practical systems. Operation of the sensor within this range allows absolute determination of the measurand on initialization.

The basic optical configuration of the low coherence interferometric network is shown in Fig. 1. The two output beams from the LCOS's are first spatially combined by the multimode fibre directional coupler and then injected into the transmission bulk Michelson interferometer (TMI). The output signal from this interferometer is then coupled into a multimode fibre network and used to illuminate the two interferometers (bulk Michelsons) acting as sensor simulators. The OPD of the TMI is then scanned by $\lambda_n/2$ (where n is 1 or 2) such that the transfer function of each sensor is scanned.

Using two optical sources, with slightly different central wavelengths (λ_1, λ_2), an effective wavelength

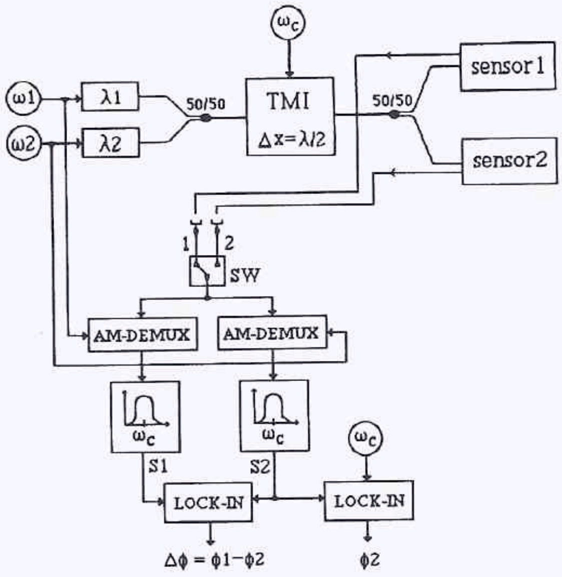

Fig. 1. Schematic arrangement of the multiplexing sensor network (with the signal processing scheme) exploiting low coherence interferometry. TMI: transmission Michelson interferometer; SW: switch for remote operation of the optical signal from each sensor, which is transferred via an optical fibre to the photodetectors.

(λ_e) is synthesized, much larger than each individual wavelength:

$$\lambda_e = \frac{\lambda_1\lambda_2}{|\lambda_2 - \lambda_1|} = \frac{\lambda_1\lambda_2}{|\Delta\lambda|}\,. \tag{1}$$

The balance position of the sensing and scanning interferometer (TMI) is determined when the outputs relative to these two wavelengths are in phase. In a conventional low coherence system, a tracking mechanism acts on the TMI to keep the balance position on the action of the measurand, which means that the in-phase condition of the two wavelengths is maintained.

In the present system the OPD of the TMI is set in an "average" value and the variation of the OPD of the sensing interferometer is determined through the phase difference of the outputs related to each wavelength. Therefore, the maximum tracking range of the system is $\pm\lambda_e/2$, which sets the scanning range of each sensor. In the case where the sensing interferometers are of the Michelson type, the measurement range is $\pm\lambda_e/4$ due to the reflective nature of the interferometer. However, the dynamic range remains the same as the sensitivity of the instrument is increased by a factor of 2.

To implement the demodulation scheme described above, as a first step, we obtain the value of the phase for each wavelength, which is given by

$$\phi_1 = (2\pi/\lambda_1)(\Delta L_{si} - \Delta L_{\mathrm{TMI}}) , \quad (2a)$$

$$\phi_2 = (2\pi/\lambda_2)(\Delta L_{si} - \Delta L_{\mathrm{TMI}}) , \quad (2b)$$

where ΔL_{si} is the OPD of the ith sensor ($i=1, 2$), which is much larger than the coherence length of either source; ΔL_{TMI} is the OPD of the scanning interferometer. Then, if the range of ΔL_{si} does not exceed $\pm\lambda_e/2$ (around $\Delta L_{si}=\Delta L_{\mathrm{TMI}}$ (average)), it is possible firstly, to compute the differential phase "$\Delta\phi$" ($\Delta\phi=\phi_1-\phi_2$) by combining Eqs. (2a) and (2b) and secondly, to readjust the result in the $[-\pi, +\pi]$ interval to obtain the value of $\Delta L=(\Delta L_{si}-\Delta L_{\mathrm{TMI}})$:

$$|\Delta L| = (\lambda_e/2\pi)|\Delta\phi| . \quad (3)$$

Using the demodulation electronics shown schematically in Fig. 1, the absolute phases of each sensor simulator can be determined, where ϕ_2 (or ϕ_1) gives the absolute optical phase (modulo 2π) and $\Delta\phi$ gives the fringe number. By modulating the PZT in the TMI with a sawtooth waveform with an amplitude of $(\lambda_2+\lambda_1)/2$, at frequency ω_c (the optimum condition), the detector signal after AM demodulation and bandpass filtering at this frequency is of the form of a heterodyne carrier where its phase is modulated by the induced phase changes in the signal. This sawtooth waveform is also used as a frequency carrier (ω_c) for the demodulation of the absolute phase of each sensor. Then, with the electronic switch SW set to select the output signal, from one of the sensors, two pseudo-heterodyne carriers, are generated which take the form:

$$S_1 \approx \cos(\omega_c t + \phi_1) , \quad (4a)$$

$$S_2 \approx \cos(\omega_c t + \phi_2) . \quad (4b)$$

Hence if these signals are fed into phase meters (lock-in) then the electronic comparison of S_1 and S_2 and ω_c and S_2 give the fringe number and absolute phase of the sensor, respectively.

3. Experimental

All interferometers used in the experiment reported here were bulk Michelson interferometers. Light from both sources was sinusoidally modulated by direct injection-current modulation at frequencies of 8 kHz and 13.3 kHz for sources λ_1 and λ_2, respectively. The sources used here were Sharp LT023 MC multimode laser diodes with central wavelengths of 781 nm and 789 nm. The average power injected into the system from each laser was ≈ 600 μW. These lasers have been designed by the manufacturer to operate in the 'self-pulsating' mode in order to minimize the effects of optical feedback on their stability [5]. The use of this source is particularly advantageous, in this application, as it is unnecessary to use optical isolators. The OPD's of the sensor simulators were set in the region of 1000 μm, corresponding to the centre of the first coherence valley of the autocorrelation function [6] of both sources, as indicated in Fig. 2. The fringe visibility at the output of each sensor was found to be ≈ 0.3 and $\lambda_e = 77$ μm; the returned power from each sensors was ≈ 12 μW. The mean OPD of the TMI was set so that it was within a few microns of the OPD of sensor 2 whilst the OPD of sensor 1 was set at ~ 20 μm with respect to sensor 2. It was seen that the outputs S_1 and S_2 (Fig. 1, S_1, S_2 corresponding to λ_1 and λ_2, respectively) derived from sensor 1 (switch at position 1, Fig. 1), were in quadrature, i.e. $\Delta\phi \approx 90°$. Changing the switch (SW) to position 2, these outputs were now in phase, i.e. $\Delta\phi \approx 0°$ (because the $\mathrm{OPD_{TMI}} \approx \mathrm{OPD_{SL}}$). Similar results were obtained when the TMI was tuned to sensor 1.

As the output from each sensor simulator was pro-

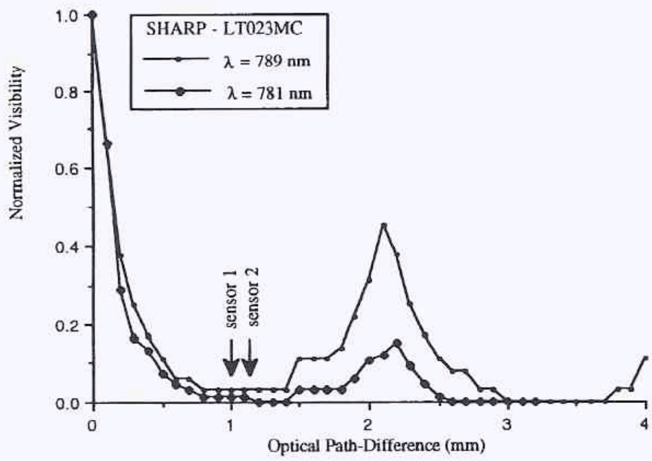

Fig. 2. Visibility functions of the Sharp multimode laser diodes. The mean operating point of the sensor simulators is also indicated.

vided by an independent output fibre link, no cross talk between the sensors was experienced. In Fig. 3 the variation of $(\phi_1-\phi_2)$ when the mirror displacement of sensor 1 was varied over its full dynamic range is shown; this data gives the fringe number. The variation of "ϕ_1" over the same range is shown in Fig. 4; the total number of fringes scanned was 115.

This data was combined to obtain the absolute value of the phase of sensor 1, which could be determined to $\sim 1°$, which means an equivalent displacement resolution of ≈ 1 nm. This phase resolution was set by electronic noise generated in the AM demodulation scheme. Considering that the working range is ≈ 45 μm, the system dynamic range is $\approx 20 \log (45\ \mu m / 1\ nm) = 92$ dB. Similar results were obtained from sensor 2. The experimental value of the working range is different from that predicted, theoretically (~ 38.5 μm) due to the uncertainties in the manufacturers quoted, values of the central wavelengths of both laser diodes, which were not temperature controlled.

4. Discussion and conclusions

The performance of the system depends on the absolute stabilities of the source wavelengths which are known to be temperature dependent. Thus, to ensure that there are no errors in the determination of the fringe number, both lasers must be temperature stabilized. By differentiating Eq. (3), we obtain the variation of the effective wavelength (λ_e) with the fringe number $(\Delta\phi)$:

$$d\lambda_e = -(\lambda_e^2/2\pi\Delta L)\, d(\Delta\phi) \tag{5}$$

and the variation of λ_e with temperature is

$$\frac{d\lambda_e}{d\Delta T} = \left(\frac{d\lambda}{dT}\right)\left(\frac{\lambda_2^2-\lambda_1^2}{\Delta\lambda^2}\right), \tag{6}$$

where it is assumed that both sources are maintained in an environment with the same temperature gradient, i.e., $d\lambda_1/dT = d\lambda_2/dT$, typical values of $d\lambda/dT$ are 0.25 nm/°C [7]. Thus, for a fringe number accuracy of 1 mrad (milliradian) and for the central wavelengths used in this system (781 nm and 789 nm), the relative temperature of the lasers, estimated using relations (5) and (6), must be maintained within 0.5°C. The accuracy also depends on the linearity of the scanning PZT in the TMI unit.

The minimum detectable phase change in the system corresponds to the condition where the detected optical signal is equal to the shot noise at the detec-

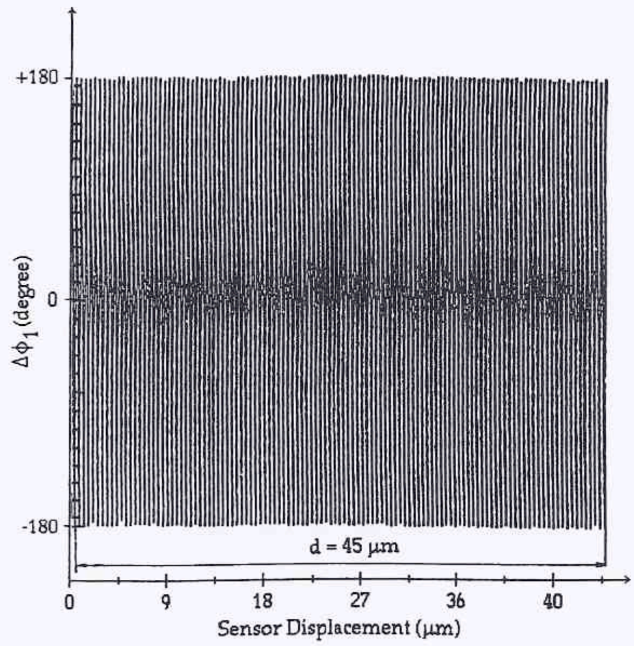

Fig. 4. Data recovered from the processing electronics showing the variation ('sawtooth') of ϕ_1 indicating the number of fringes (=115) over the full working range.

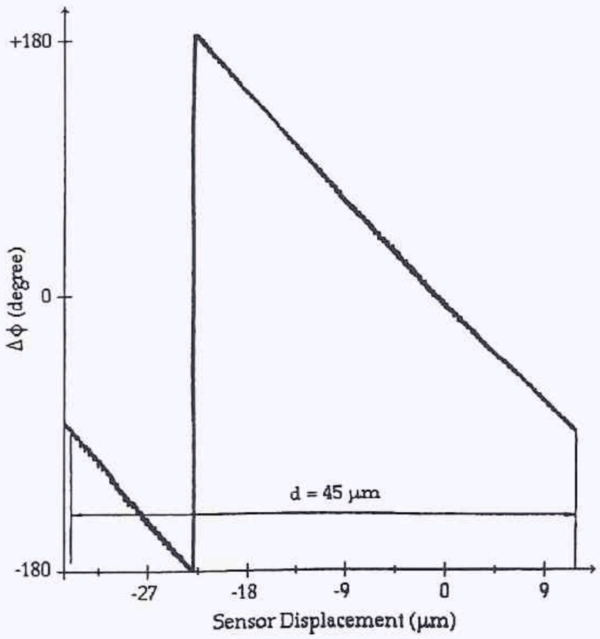

Fig. 3. Data recovered from the processing electronics showing the sawtooth variation of $(\phi_1-\phi_2)$ as the displacement of sensor simulator is varied over the full working range.

tor, for detected powers of $\approx \mu W$ phase changes of $\approx \mu rad/\sqrt{Hz}$ at signal frequencies > 10 Hz can be detected [8] (under ideal conditions). The system described here is for practical applications where the sensitivity will be determined by factors such as environmental noise and $1/f$ noise, particularly at low frequencies, we therefore choose to operate the system at a modest resolution of ≈ 1 mrad/$\sqrt{Hz}$ (equivalent to a phase resolution of $\approx 1°$) as it is readily obtainable with conventional electronic processing such as lock-in amplifiers or phase meters. The large dynamic range being achieved by the use of the dual wavelength technique.

One major advantage of operating at low phase resolution is that if the number of sensors were increased, whilst the input power remains constant, the range to resolution of all the sensors would be unaffected. For example, if we expanded the network to eight sensors, then the returned power per sensor (assuming the sensors were deployed in a 'tree topology' with the same loss per coupler, etc.) would be reduced to ≈ 1–2 μW, again giving a shot noise performance of $\approx \mu rad/\sqrt{Hz}$, well in excess of the phase resolution required.

In conclusion, a partially multiplexed fibre optic based sensor network with low coherence dual wavelength signal processing has been demonstrated. Considering that each sensor has its own return fibre, this system allows the outputs of several sensors to be simultaneously demodulated assuming that the OPD of the sensors are not different by an amount larger than λ_e. Also the crosstalk between sensors is virtually eliminated.

Acknowledgements

This work was partially funded by the SERC/DTI Nanotechnology link scheme. Antonio Ribeiro also acknowledges the financial support of the Optoelectronics Group at INESC-Porto, Portugal and the Treaty of Windsor programme.

References

[1] A.S. Gerges, F. Farahi, T.P. Newson, J.C.D. Jones and D.A. Jackson, Electron. Lett. 23 (1987) 1110.

[2] J.L. Brooks, R.W. Wentworth, R.C. Youngquist, M. Tur, B.Y. Kim and H.J. Shaw, J. Lightwave Tech. 3 (1985) 1062.

[3] J.L. Brooks, B. Moslehi, B.Y. Kim and H.J. Shaw, J. Lightwave Tech. 5 (1987) 1014.

[4] A.D. Kersey and A. Dandridge, Proc. SPIE in Fibre Optic Sensors II, SPIE vol. 798 (1987) 176.

[5] S. Yamashita, A. Ohishi, T. Kajimura, M. Inque and Y. Fukui, IEEE J. Quantum Electron. 25 (1989) 1483.

[6] A.S. Gerges, T.P. Newson and D.A. Jackson, Appl. Optics 29 (1990) 4473.

[7] H.C. Casey, Jr. and M.B. Panish, eds. Heterostructure Lasers, (Academic, Orlando, 1978).

[8] D.A. Jackson and J.D.C. Jones, Optical Fibre Sensors, eds. B. Culshaw and J. Dakin (Artech House Publishing, 1989), Ch. 10.